Electronic Supplementary Material

Synergistically interactive P–Co–N bonding states in cobalt phosphide-decorated covalent organic frameworks for enhanced photocatalytic hydrogen evolution

Lumei Huang,[a,b] Dengke Wang,*[b] Honghu Zeng,[a] Lingling Zheng,[b] Shiqin Lai,[b] and Jian-Ping Zou*[a,b]

[a] *College of Environmental Science and Engineering, Guilin University of Technology, Guilin 541004, P. R. China*

[b] *Key Laboratory of Jiangxi Province for Persistent Pollutants Control and Resources Recycle, Nanchang Hangkong University, Nanchang 330063, P. R. China*

E-mail: dengkewanglab@qq.com (D. Wang), zjp_112@126.com (J. Zou)

Experimental section

1 Materials

Trichlormethane ($CHCl_3$，99.5%) was provided from Nanchang XinGuang Co.. Triflic acid (98%), anhydrous $ZnC1_2$ (98%) and NaH_2PO_2 were obtained from Macklin (China, Shanghai). N,N-dimethyl formamide (DMF, 99%) and chloroplatinic acid ($H_2PtCl_6 \cdot 6H_2O$) were acquired from Aldrich (China, Shanghai). Cobalt nitrate ($Co(NO_3)_2$) and cetyltrimethylammonium bromide (CTAB) were provided by Shanghai Chemical Reagent Co., Ltd. (China, Shanghai). Ethylene glycol and Urea were obtained from Xilong Chemical Co., Ltd. (China, Guangdong).

2 Synthesis of covalent triazine-based frameworks (CTF-1)

CTF-1 was synthesized following a previously reported method with slight modifications. Typically, trifluoromethanesulfonic acid (19.96 g, 133.0 mmol) was added into a pre-dried three-neck round bottom flask containing $CHCl_3$ (30 mL) under inert gas atmosphere. Then, 1,4-dicynobenzene (4.26 g, 33.25 mmol) dissolved in $CHCl_3$ (200 mL) was slowly dropwised into above resulted mixture at 0 ℃ under vigorous stirring. The mixture was continuously stirred at 0 ℃ for 2 h and then heated to 40 ℃ for 48 h. A solid precipitate turned from colorless to yellow was formed. After cooled down to room temperature, the solid precipitate was rapid added to 660 mL of deionized water containing 34 mL of ammonia solution (25%), and then stirred for 2 h. The precipitate was obtained by filtration and washed successively with deionized water, ethanol, acetone and chloroform, respectively. The yellow product was dried under vacuum overnight at 60 ℃. The yellow precipitate regards as pre-CTF. Pre-CTF (2.100 g, 16.39 mmol) was thoroughly mixed with $ZnCl_2$ (1.787 g, 13.11 mmol) and transferred to a porcelain crucible with lid, and then treated at 400 ℃ for 10 min with a ramping rate of 2.5 ℃/min under argon atmosphere in a tube furnace. After cooling to room temperature under argon atmosphere, the crude products were grounded and stirred in deionized water (150 mL) for 12 h at 60 ℃, filtered and washed thoroughly with water to remove the majority of the salt. The mixtures were further stirred in 0.1 M

HCl (150 mL) for 12 h at 60 ℃ to remove the residual $ZnCl_2$ filtered and subsequently washed with water and tetrahydrofuran. The product was dried under vacuum for 12 h at 60 ℃.

3 Characterization

X-ray diffraction (XRD) patterns were collected on a D8 Advance X-ray diffractometer (Bruker, Germany) with Cu Kα radiation (λ= 1.5406 Å). The accelerating voltage and the applied current were 40 kV and 40 mA, respectively. Data were recorded in a scan mode with a scanning speed of 2 °/min in the 2 θ range between 5° and 60°. UV–vis diffuse reflectance spectra (UV-vis DRS) of the powers were obtained with $BaSO_4$ used as a reflectance standard. Fourier transformed infrared (FTIR) spectra of the samples were performed by a VERTEX-70 spectrometer, and KBr was used as a blank control. The scanning electron microscopy (SEM) images were collected with a Nova Nano SEM 230 microscopy (FEI, Hillsboro, OR, USA). The transmission electron microscopy (TEM) and high-resolution transmission electron microscopy (HRTEM) images were obtained on JEOL model JEM 2010 EX instrument. CoP size distribution was obtained using Nano Measurer software. Brunauer–Emmett–Teller (BET) surface area of samples were measured by means of N_2 adsorption over a NOVA 2000e (Quantachrome) equipment. The element composition of catalysts was identified by X-ray photoelectron spectroscopy (XPS) (VG 250 Escalab spectrometer and Al-K =1486.7 eV). All binding energy were referenced to the C 1s peak at 284.8 eV of the surface adventitious carbon. Photoluminescence (PL) spectra were carried out on a fluorescence spectrometer (Hitachi F-4500), which used a 325 nm wavelength as the excitation source. Time-resolved fluorescence decay spectroscopy was measured using a time correlated single-photon counting system (FS5 Spectrofluorometer, Edinburgh Instruments) which used a 380 nm picosecond pulsed diode laser (EPLED-380, Max Average Power 40 μW) as the excitation source. Inductively coupled optical emission spectrometer (ICP-OES) was performed on Optima 8000 (PerkinElmer). Before ICP-OES experiment, the sample was digested in mixture of HNO_3 and milli-Q water.

4 Apparent quantum yield calculation

To evaluate the wavelength dependence of the photocatalyst, the apparent quantum yield (AQY) for H_2 evolution was detected equipped with several band-pass filters of Full width at half maximum (FWHM)=15 nm under a 300 W Xe lamp irradiation. The average intensity of irradiation was determined by a Radiometer (FZ-A, Photoelectric Instrument Factory of Beijing Normal University). The AQY was calculated according to the following equation.

$$\mathrm{AQY}(\%) = \frac{2\times\text{number of evolved } H_2 \text{ molecules}}{\text{the number of incident photons}} \times 100\%$$

$$\text{The number of incident photons} = [I\times S]/[E]$$

$$E = h\nu = h\,\frac{c}{\lambda}$$

I: light intensity S: the irradiated area of reactor

E: the photon energy h: the Planck constant

c: indicates speed of light λ: the wavelength

5 Density functional theory (DFT) calculations

We have employed the first-principles to perform all density functional theory (DFT) calculations within the generalized gradient approximation (GGA) using the Perdew-Burke-Ernzerhof (PBE) formulation.[1] The projected augmented wave (PAW) potentials to describe the ionic cores and take valence electrons into account using a plane wave basis set with a kinetic energy cutoff of 450 eV. Partial occupancies of the Kohn−Sham orbitals were allowed using the Gaussian smearing method and a width of 0.05 eV. The electronic energy was considered self-consistent when the energy change was smaller than 10^{-5} eV. A geometry optimization was considered convergent when the energy change was smaller than 0.05 eV/Å. Grimme' s DFT-D3 methodology was used to describe the dispersion interactions. The Brillourin zone was sampled with 2×2×1 through the computational process.

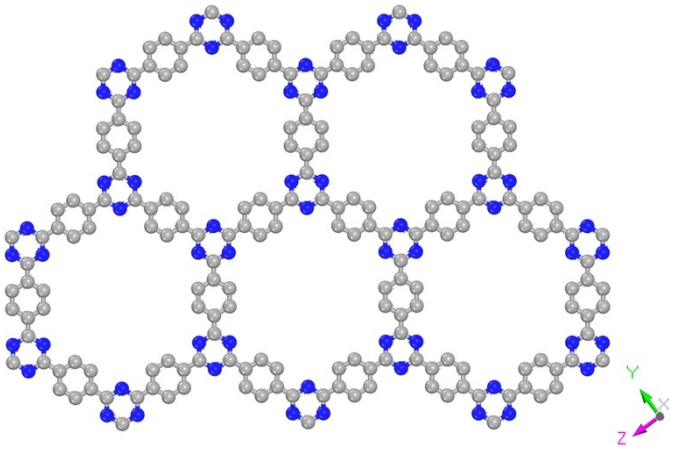

Fig. S1 The view of the structure of CTF-1 along the x axis: nitrogen (blue), carbon (gray).

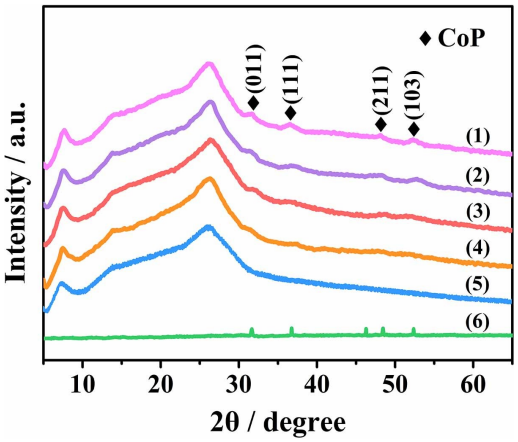

Fig. S2 XRD patterns of (1) CTF-CoP-5%, (2) CTF-CoP-3%, (3) CTF-CoP-1%, (4) CTF-CoP-0.5%, (5) CTF-1 and (6) CoP.

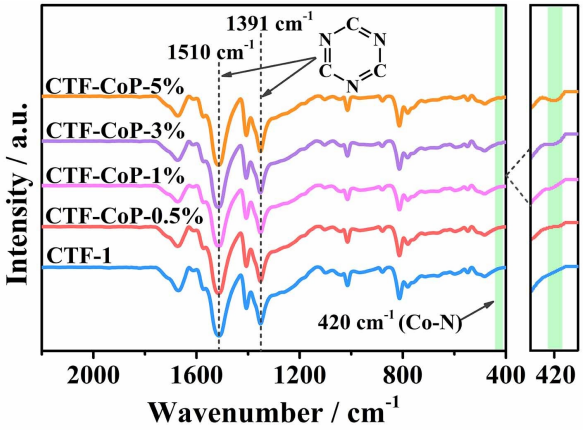

Fig. S3 FTIR patterns of CTF-1 and CTF-CoP with different amount of CoP.

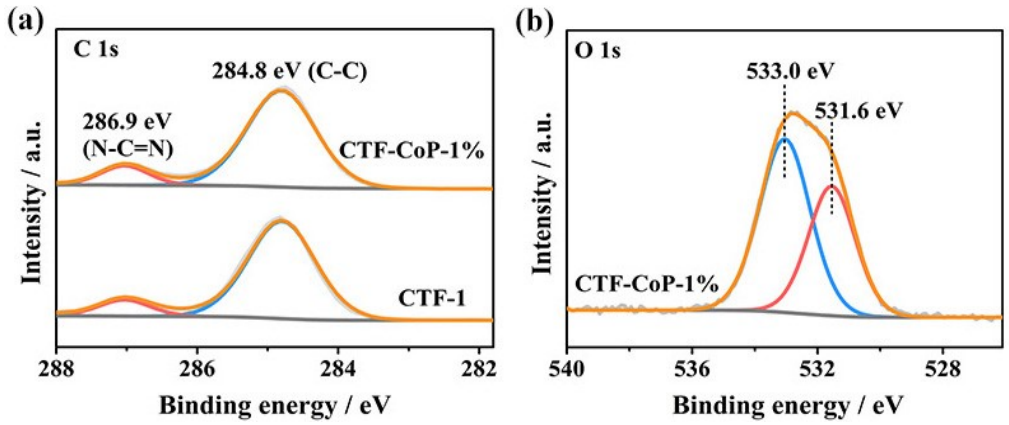

Fig. S4 XPS spectra of (a) C 1s regions of CTF-CoP-1% and CTF-1, (b) O 1s region of CTF-CoP-1%.

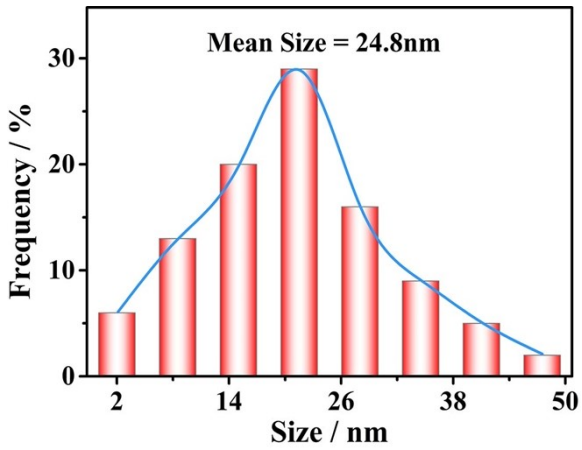

Fig. S5 CoP size distribution histogram of CTF-CoP-1%.

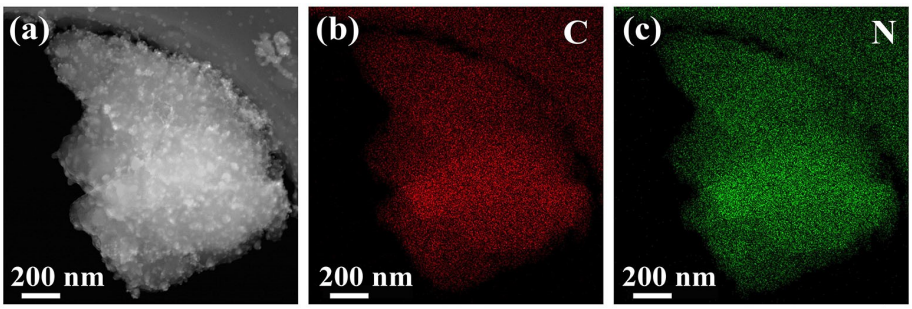

Fig. S6 (a) HRTEM image of CTF-CoP-1%; EDX elemental mapping of (b) C and (c) N of CTF-CoP-1%.

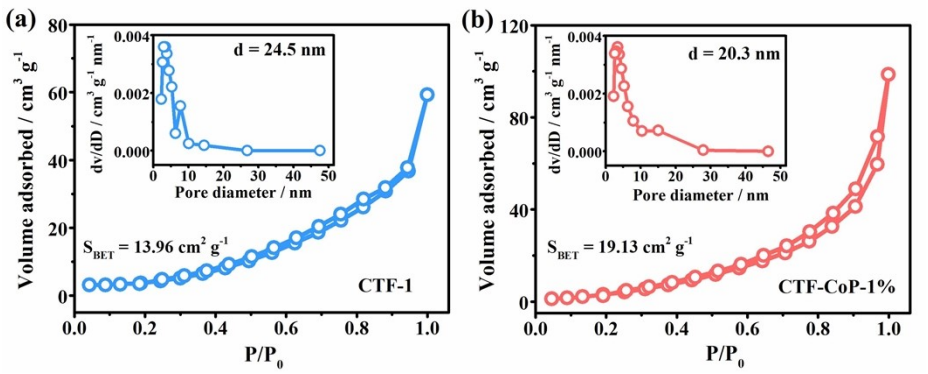

Fig. S7 N_2 adsorption-desorption isotherms and the Barrett-Joyner-Halenda (BJH) pore size distributions (inset) of (a) CTF-1 and (b) CTF-CoP-1%.

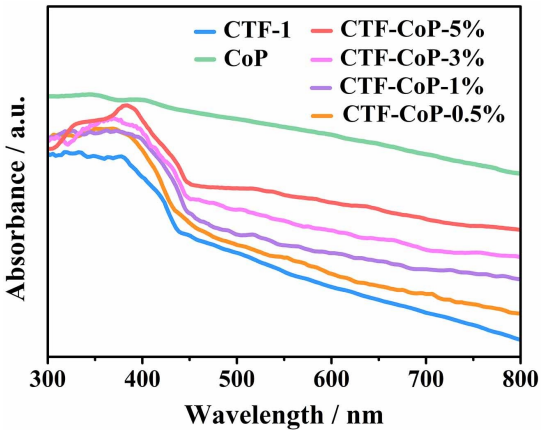

Fig. S8 UV-vis DRS spectra of the samples.

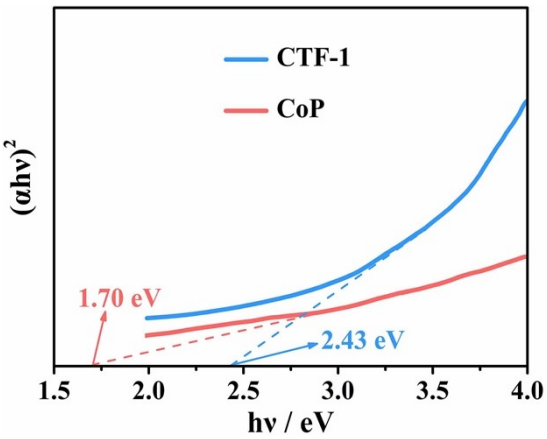

Fig. S9 UV-vis diffuse reflectance the plots of $(\alpha h\nu)^2$ vs $h\nu$ over CTF-1 and CoP.

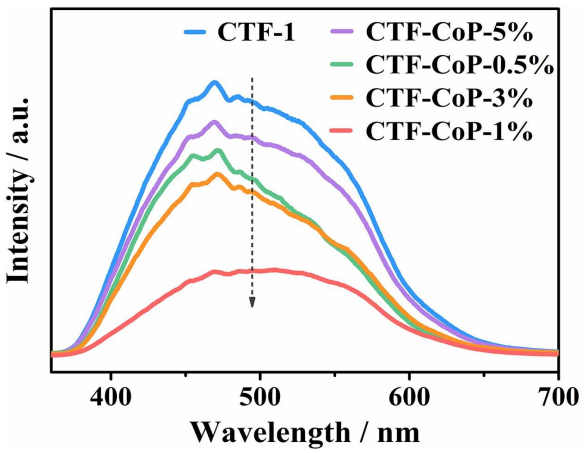

Fig. S10 Room temperature PL spectra of the synthesized samples.

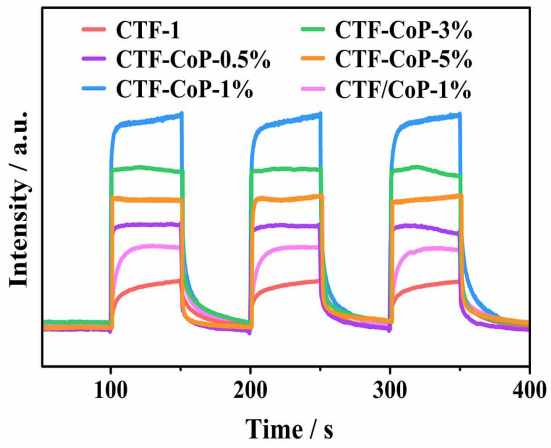

Fig. S11 Transient photocurrent responses of the as-prepared samples.

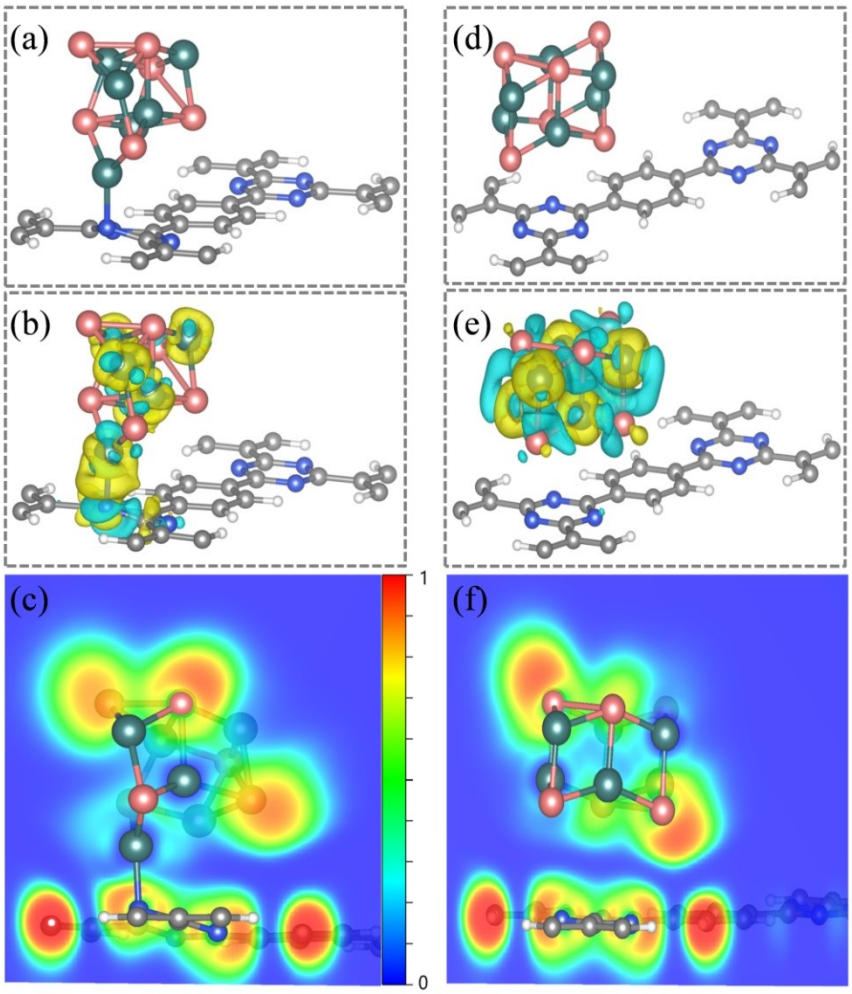

Fig. S12 (a and d) Optimal structure, (b and e) difference charge density and (c and f) electronic location function of CTF-CoP and CTF/CoP, respectively.

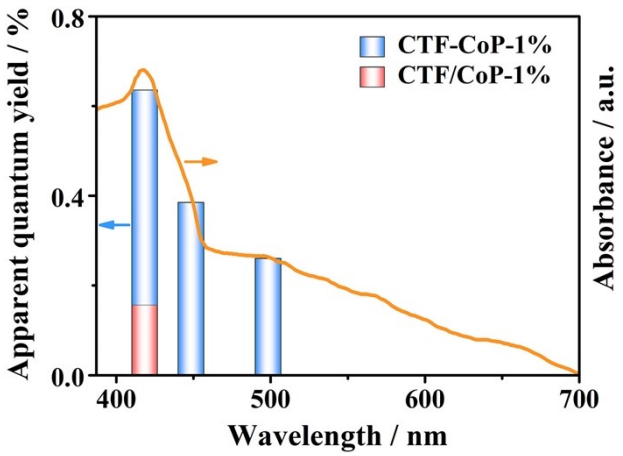

Fig. S13 Wavelength-dependent apparent quantum yield of H_2 evolution over the CTF-CoP-1% and CTF/CoP-1%.

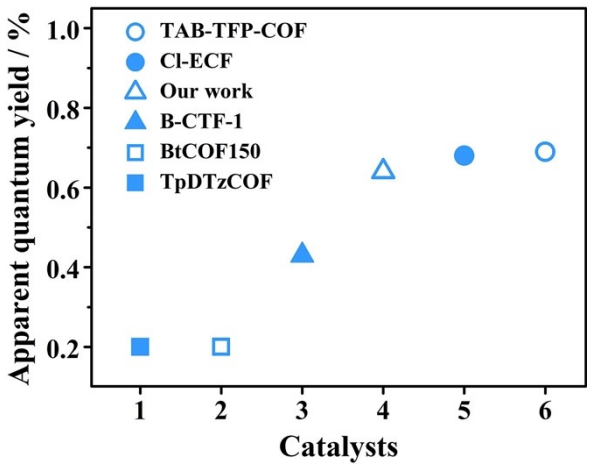

Fig. S14 Comparison diagram of AQY values reported in literature and this work.

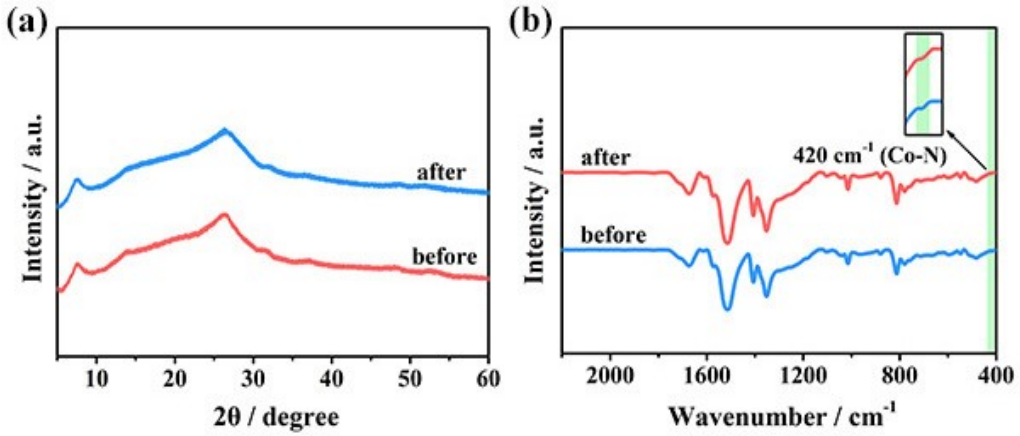

Fig. S15 (a) XRD patterns and (b) FTIR patterns of CTF-CoP-1% sample before and after 16 h photocatalytic reaction.

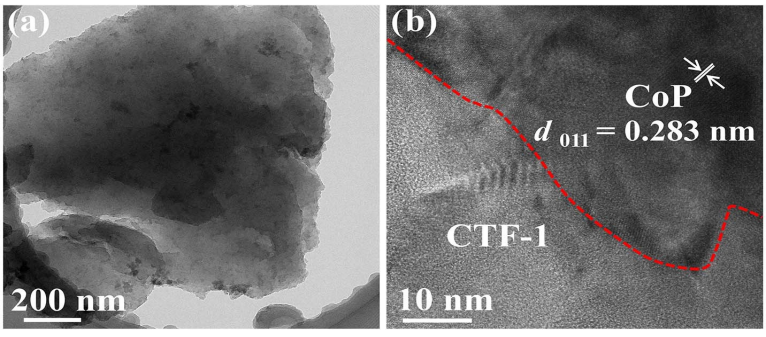

Fig. S16 TEM image (a) and HRTEM image (b) of CTF-CoP-1% after 16 h photocatalytic reaction.

Table S1 Exponential decay-fitted parameters of fluorescence lifetime of different samples.

Sample	A_1	A_2	τ_1 (ns)	τ_2 (ns)	τ_{ave}(ns)
CoP	0.256	0.027	0.42	2.18	1.04
CTF-1	0.221	0.029	0.53	2.79	1.45
CTF/CoP-1%	0.219	0.031	0.67	3.48	1.86
CTF-CoP-1%	0.197	0.033	0.78	4.14	2.36

Note:

The tri-exponential functionas follows:

$$R(t) = A_1 \exp(-t/\tau_1) + A_2 \exp(-t/\tau_2) \qquad (1)$$

Meanwhile, the average lifetime (τ_{ave}) was calculated using following equation.

$$\tau_{ave} = \frac{\tau_1^2 A_1 + \tau_2^2 A_2}{\tau_1 A_1 + \tau_2 A_2} \qquad (2)$$

where τ_1, and τ_2 are the emission lifetimes, and A_1, and A_2 are the corresponding amplitudes. In general, the longer decay lifetime component τ_1 is considered to free exciton recombination in the CTF-1 and its composites, and the shorter decay lifetime components τ_2 are ascribed to the surface-related nonradiative recombination of the charge carriers.

Table S2 The apparent quantum yield of H_2 evolution over the CTF-CoP-1% and CTF/CoP-1% at different incident wavelengths.

Sample	λ =420 nm	λ =450 nm	λ =500 nm
CTF/CoP-1%	0.16 %	—	—
CTF-CoP-1%	0.64%	0.39%	0.26%

Reference

1 G. Kresse, J. Furthmüller, *Comput. Mater. Sci.*, 1996, **6**, 15−50.

2 X. Wu, M. C. Zhang, Y. S. Xia, C. L. Ru, P. Y. Chen, H. Zhao, L. Zhou, C. L. Gong, J. C. Wu and X. B. Pan, *J. Mater. Chem. A*, 2022, **10**, 17691-17698.

3 S. Li, M. F. Wu, T. Guo, L. L. Zheng, D. K. Wang, Y. Mu, Q. J. Xing and J. P. Zou, *Appl. Catal. B: Environ.*, 2020, **272**, 118989.

4 L. L. Zheng, L. S. Zhang, Y. Chen, L. Tian, X. H. Jiang, L. S. Chen, Q. J. Xing, X. Z. Liu, D. S. Wu and J. P. Zou, *Chinese J. Catal.*, 2021, **43**, 811-819.

5 S. Ghosh, A. Nakada, M. A. Springer, T. Kawaguchi, K. Suzuki, H. Kaji, I. Baburin, A. Kuc, T. Heine, H. Suzuki, R. Abe and S. Seki, *J. Am. Chem. Soc.* 2020, **142**, 9752-9762.

6 B. P. Biswal, H. A. Vignolo-González, T. Banerjee, L. Grunenberg, G. Savasci, K. Gottschling, J. Nuss, C. Ochsenfeld and B. V. Lotsch, *J. Am. Chem. Soc.*, 2019, **141**, 11082-11092.